

A 163 MICRON LASER HETERODYNE RADIOMETER FOR OH:

PROGRESS REPORT

H. M. Pickett and T. L. Boyd
Jet Propulsion Laboratory

ABSTRACT

We are currently developing a 163 micron (1.836 THz) radiometer for airplane and/or balloon platforms.

The laser local oscillator is a CO₂ pumped methanol laser operating at frequency which is ~ 1 GHz from the $J = 3/2 - 1/2$ transition of OH. The laser will be used directly as a local oscillator or will be translated in frequency to closer coincidence with the OH emission, depending on achieved detector I.F. bandwidth. Frequency translation techniques which will be described are diode mixing and a new method of single sideband generation using an external Stark modulated gas cell.

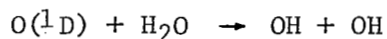
The photoconductive mixer which will be used is a strained Ge crystal, doped with Ga, originally used as an incoherent detector. The uniaxial strain on the Ga doped Ge crystal shifts the threshold for photoconduction from 100 cm^{-1} to frequencies as low as 50 cm^{-1} . These detectors are currently being characterized as mixers in the laboratory. Of particular interest are the effect of local oscillator power and strain on I.F. bandwidth, detector impedance and conversion loss. Preliminary results of these tests will be described and compared with theoretical expectations.

INTRODUCTION

The hydroxyl radical (OH) is recognized as a keystone species for the understanding of ozone destruction in the stratosphere. As Wofsy has stated (ref. 1),

"The OH radicals.....drive most of the photochemistry of the stratosphere. They play a pivotal role in the partitioning of NO_x and ClO_x among species which are relatively reactive or stable toward O₃ and O."

The OH radical plays a catalytic role in the HO_x cycle. In addition, increased OH would reduce the importance of the NO_x cycle but would increase the importance of the ClO_x cycle (ref. 2). The major source of OH is the reaction of O(¹D) with water:



In the region below 80 km, the main source of $O(^1D)$ is the photolysis of ozone (ref. 3). As a consequence, OH concentration is a maximum at ~ 50 km. The region near 50 km is important for checking on the quantity of OH produced, while the region of 20-40 km is important for determining the relative roles of the chlorine and nitrogen cycles.

The OH submillimeter wavelength rotational lines provide an excellent probe of OH, particularly when remote sensing emission measurements are used. Figure 1 shows the emission of OH calculated for a balloon platform looking horizontally at an altitude of 40 km. Most of the emission shown comes from higher altitude. Calculated emission from an airplane flying at 12 km would be quite similar. Emission from lower altitudes is broader because of increased air pressure and is expected to be weaker because of decreased OH abundance. This particular OH transition is the lowest frequency set of rotational lines and happens to be quite close to a methanol laser line. In figure 2 it can be seen that several of the lines are within 1 GHz of the laser transition. This fortunate coincidence forms the basis for our 1.8 THz radiometer. It might be noted that these lines have recently been observed in the stratosphere by Kendall and Clark (ref. 4) using a Michelson interferometer on a balloon platform. However, for detailed altitude distributions of OH, a heterodyne system will be needed.

LOCAL OSCILLATOR

The block diagram of our radiometer is shown in figure 3. It consists of the usual combination of mixer, local oscillator, and filter bank. If the mixer has a bandwidth in excess of 1 GHz, the laser can be used directly as the local oscillator. However, it is quite likely that the bandwidth of our mixer will be smaller than 1 GHz and a scheme for frequency shifting the laser is needed. The scheme we are planning involves a modulation of the laser followed by filtering of the lower modulation sideband. This modulator and sideband filter are therefore part of the local oscillator system. A number of groups have been active in generating sidebands using an R.F. biased diode (e.g. ref. 5). The efficiency of sideband generation using this method is not large but the offsets achievable are limited only by the optical coupling structure for the diode.

An alternative modulation method we have been investigating involves modulation of absorption in an external gas cell. Surprisingly such a technique can generate in a single sideband mode with up to 10% efficiency. The method is best illustrated by a model experiment we performed at 104 GHz using a methyl fluoride absorption (ref. 6.). The block diagram of the spectrometer system used is shown in figure 4. There is a source klystron locked to 102 GHz and a local oscillator klystron locked to a frequency

which is exactly 1140 GHz below the source klystron. The mixer and spectrum analyzer combine to make a very high resolution radiometer for power leaving the sample cell. The methyl fluoride pressure in the sample cell was ~ 80 mtorr and the 10.8 MHz electric field had an amplitude of 40 V/cm. This field modulates the absorption frequency by 14 MHz. The modulation frequency was significantly larger than the 1.5 MHz width of the methyl fluoride absorption. The results of this experiment are shown in figure 5. Trace B, taken when the input signal was on resonance with the absorption shows the sideband pattern expected for amplitude modulation. When the input is above or below resonance, the effect of the modulated absorption is to put enhanced power in the sideband located on the other side of the absorption center. In this experiment, the absorptivity of the sample was small and the sideband level only reached the 5 db level. However, for stronger absorption, the theoretical model of the experiment predicts that the sideband level can approach 10 db.

THE MIXER

Recently we have been centering most of our attention on the mixer, since the mixer characteristics drive many of the decisions about local oscillator requirements and achievable signal to noise figure. The mixer which we are testing is a strained Gallium doped Germanium crystal which is used in a photoconductive mode. Incoherent detectors of this type have been described (ref. 7), but their mixer properties have not been evaluated. We are currently evaluating the bandwidth of several mixer crystals at 96μ , 118μ and 163μ in the stressed and unstressed conditions. At this point we can only report that the bandwidth in all cases is in excess of 5 MHz based on time response tests. The material used is supplied to us by Santa Barbara Research Corp. and is only lightly compensated. The crystals are in the form of cubes 3mm on a side and are doped to a level of $\sim 10^{14}/\text{cm}^3$. Measurements of I.F. noise bandwidth by mixing a black body with the laser are currently under way.

We have also measured the D.C. photo-resistance at laser power levels in an attempt to determine the maximum achievable conversion gain of the mixer. An example of such a photo-resistance curve is shown in figure 6. As can be seen, the curve fits a simple power saturation law. This saturation behavior is reasonable if the negatively ionized acceptor concentration is not a function of the power level. At higher power levels the ionized acceptor concentration should increase due to the production of photo-holes significantly in excess of the dark ionized acceptor level. This increased ionized acceptor level will 1) increase the recombination rate and 2) decrease the mobility. The first effect occurs because the recombination rate is proportional to both ionized acceptor concentration and hole concentration, and the second effect occurs because of increased scattering by ionized acceptors relative to neutral acceptors. Both effects will slow the saturation rate with increased power, and such a trend can be seen at the higher power levels in figure 6. The conversion gain is obtainable from the

photoresistance by

$$G = 2 \left(\frac{dR}{dP} \right)^2 I_b^2 R^{-1} P \quad , \quad (1)$$

in which I_b is the bias current. The maximum gain then appears at $P = P_0/2$, with

$$G_{\max} = \left(I_b^2 R_0 / P_0 \right) \times 0.296 \quad (2)$$

in which R_0 is the dark resistance. It is possible to make $I_b^2 R_0$ on the order of P_0 , but higher bias levels suffer from the severely non-linear I-V characteristics of the crystals (see ref. 7). To achieve the high gain of eq. (2), the I.F. amplifier has to be matched to an impedance of $\sim 28 \text{ k}\Omega$. This is a problem with conventional $50 \text{ }\Omega$ amplifiers but is quite well suited to FET input amplifiers at moderate I.F. frequencies.

REFERENCES

1. Wofsy, S. C.: Temporal and Latitudinal Variations of Stratospheric Trace Gases: A Critical Comparison Between Theory and Experiment. *J. Geophys. Res.*, vol. 83, 1978, pp.364-378.
2. Crutzen, P. J.; Isaksen, I.S.A.: and McAfee, J.R.: Impact of the Chlorocarbon Industry on the Ozone Layer. *J. Geophys. Res.*, vol. 83, 1978, pp. 345-363.
3. Vlasov, M. N.: Photochemistry of Excited Species, *J. Atm. Terr. Phys.*, vol. 38, 1976, pp. 807-820.
4. Kendall, D. J. W.; and Clark, T. A.: Stratospheric Observation of Far I.R. Pure Rotational Lines of Hydroxyl, *Nature*, vol. 283, 1980, pp. 57-58.
5. Bicanic, D. D.; Zuidberg, B. F. J.; and Dymanus, A.: Generation of Continuously Tunable Laser Sidebands in the Submillimeter Region, *Appl. Phys. Lett.*, vol. 32, 1978, pp. 367-369.
6. Pickett, H. M.: The Physical Basis for Absorption of Light, *Nature*, vol. 279, 1979, pp. 224-225.
7. Kayanskii, A. G.; Richards, R. L.; and Haller, E. E.: Far Infrared Photoconductivity of Uniaxially Stressed Germanium, *Appl. Phys. Lett.*, vol. 31, 1977, pp. 496-497.

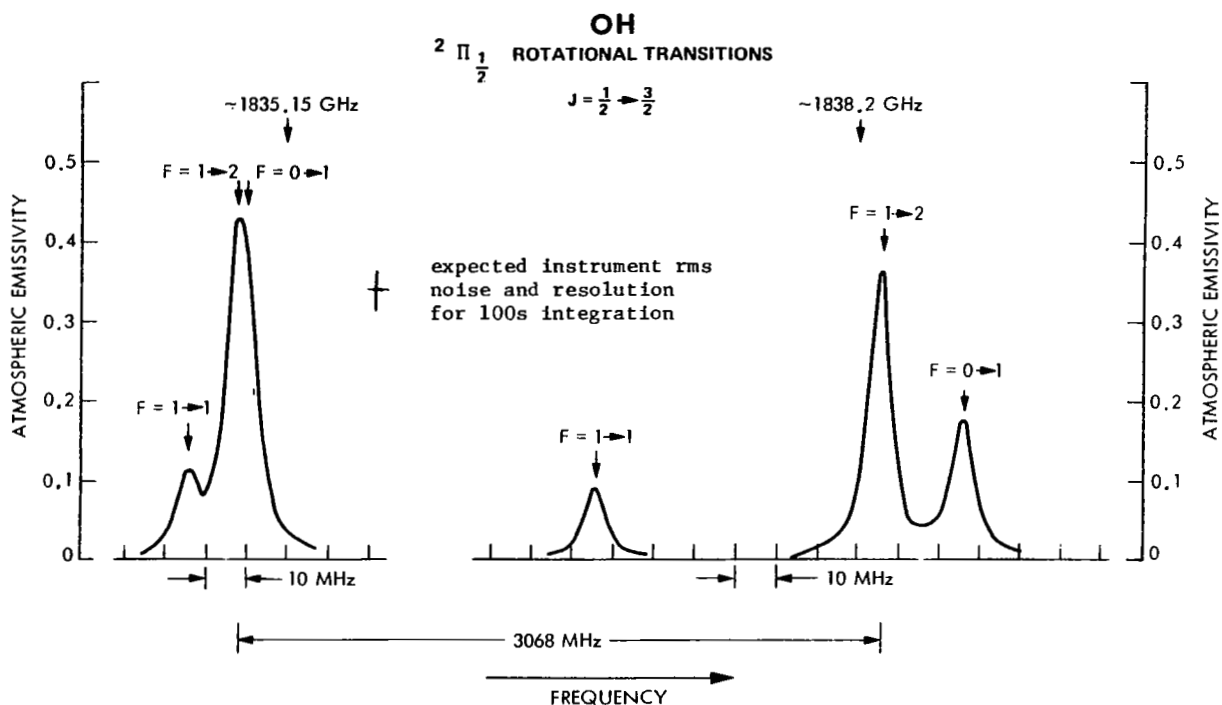


Figure 1.- Calculated emission by OH in Earth's upper atmosphere.

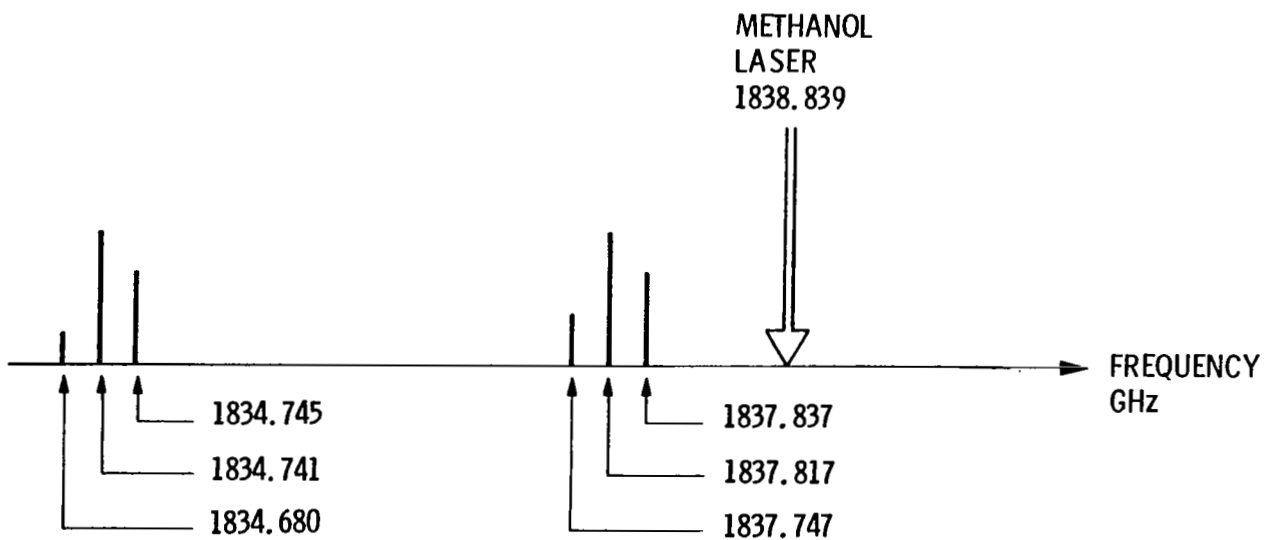


Figure 2.- OH spectrum near 1800 GHz.

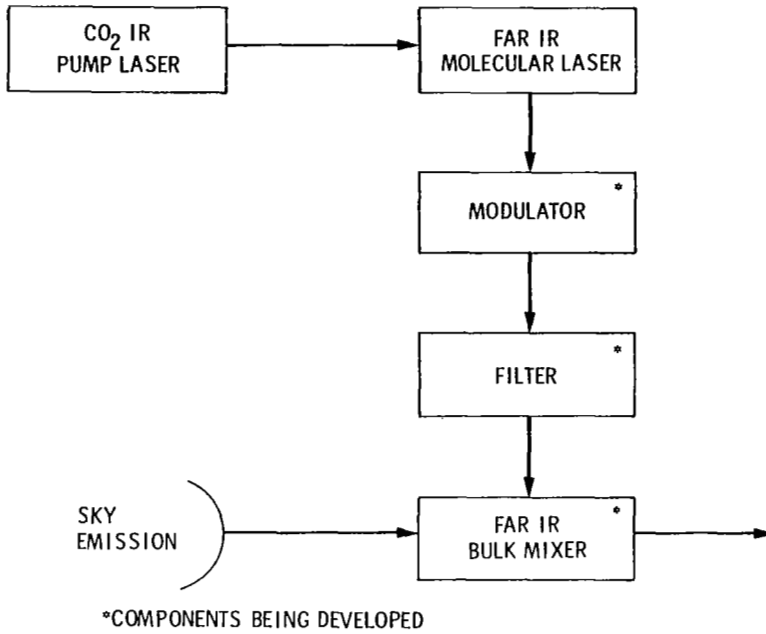


Figure 3.- 1800 GHz OH radiometer.

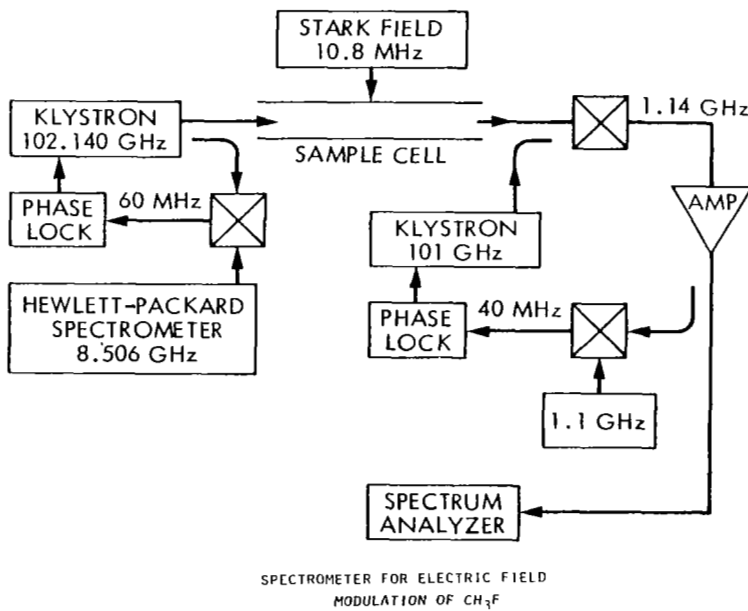
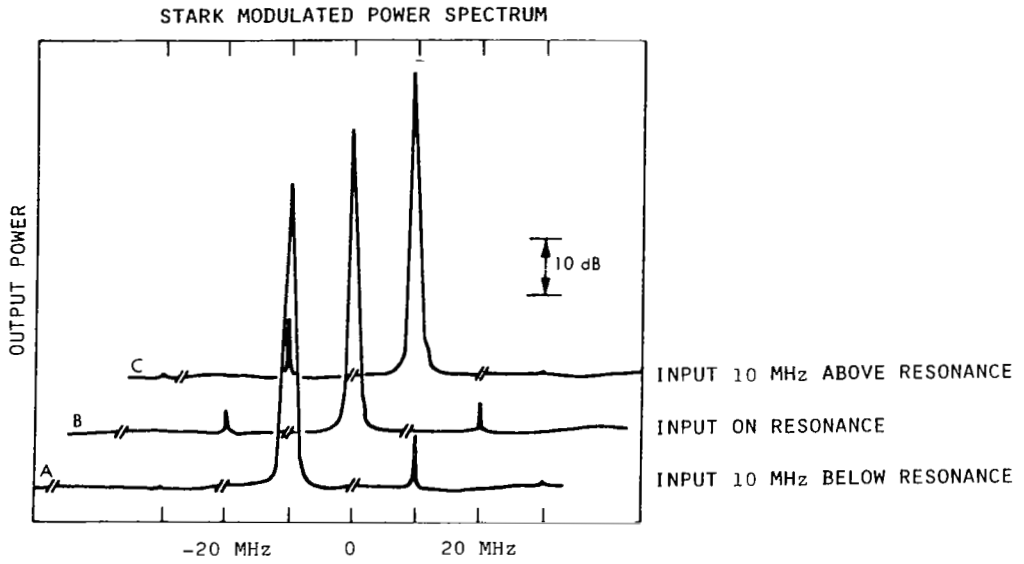


Figure 4.- Laboratory test of modulation scheme.



FREQUENCY OFFSET FROM MOLECULAR RESONANCE OF CH_3F AT 102.140 GHz

Figure 5.- New insights into the physics of light absorption. Measured asymmetry in modulated power requires light absorption to be treated as stimulated emission, not as amplitude absorption.

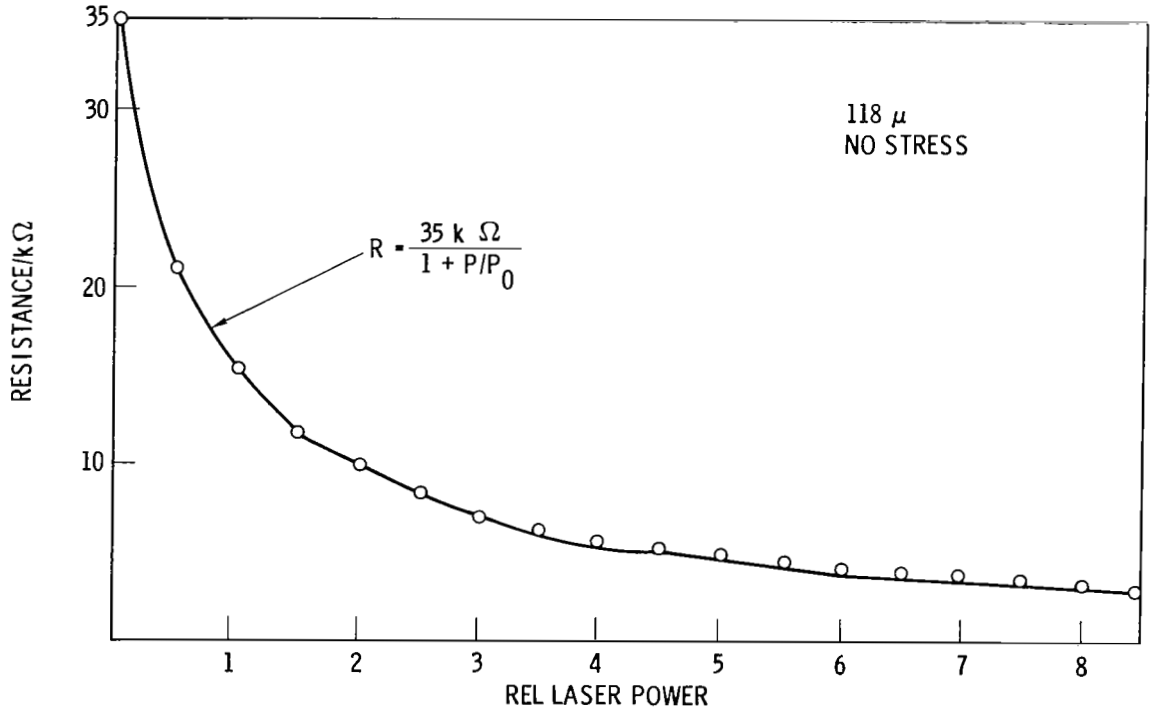


Figure 6.- Photoresistance.